

Electronic Supplementary Information

The Impact of Cyclometalated and Phosphine ligands on the Luminescence Properties of Cycloplatinated(II) Complexes: Photophysical and Theoretical Investigations

Hamid R. Shahsavari,* Sareh Pazresh

Department of Chemistry, Institute for Advanced Studies in Basic Sciences (IASBS), 444 Prof. Yousef Sobouti Blvd., Zanjan, 45137-66731, Iran; Tel: +98 243 315 3206; Fax: +98 243 315 3232; Email: shahsavari@iasbs.ac.ir (H.R.S).

Contents:	Page
Figure S1. ^1H NMR spectrum of A in CDCl_3 .	S3
Figure S2. $^{19}\text{F}\{^1\text{H}\}$ NMR spectrum of A in CDCl_3 .	S3
Figure S3. $^{195}\text{Pt}\{^1\text{H}\}$ NMR spectrum of A in CDCl_3 .	S4
Figure S4. ^1H NMR spectrum of 1a in CDCl_3 .	S4
Figure S5. $^{19}\text{F}\{^1\text{H}\}$ NMR spectrum of 1a in CDCl_3 .	S5
Figure S6. $^{31}\text{P}\{^1\text{H}\}$ NMR spectrum of 1a in CDCl_3 .	S5
Figure S7. $^{195}\text{Pt}\{^1\text{H}\}$ NMR spectrum of 1a in CDCl_3 .	S6
Figure S8. ^1H NMR spectrum of 1b in CDCl_3 .	S6
Figure S9. $^{19}\text{F}\{^1\text{H}\}$ NMR spectrum of 1b in CDCl_3 .	S7
Figure S10. $^{31}\text{P}\{^1\text{H}\}$ NMR spectrum of 1b in CDCl_3 .	S7
Figure S11. $^{195}\text{Pt}\{^1\text{H}\}$ NMR spectrum of 1b in CDCl_3 .	S8
Figure S12. HR ESI-Mass spectrum of A . Inset shows the calculated pattern.	S8
Figure S13. HR ESI-Mass spectrum of 1a . Inset shows the calculated pattern.	S9
Figure S14. HR ESI-Mass spectrum of 1b . Inset shows the calculated pattern.	S9
Figure S15. Molecular structure of A .	S10
Figure S16. Molecular structure of 1b .	S10
Figure S17. View of the optimized structure of A in gas phase (S_0) with atom numbering.	S11
Figure S18. View of the optimized structure of 1a in gas phase (S_0) with atom numbering.	S11
Figure S19. View of the optimized structure of 1b in gas phase (S_0) with atom numbering.	S12

Figure S20. View of the optimized structure of 2a in gas phase (S_0) with atom numbering.	S12
Table S1. Selected bond distances (\AA) and angles (deg) for the calculated (S_0 and T_1 in gas phase and S_0 in CH_2Cl_2) structure of A .	S13
Table S2. Selected bond distances (\AA) and angles (deg) for the calculated (S_0 and T_1 in gas phase and S_0 in CH_2Cl_2) structure of 1a .	S13
Table S3. Selected bond distances (\AA) and angles (deg) for the calculated (S_0 and T_1 in gas phase and S_0 in CH_2Cl_2) structure of 1b .	S14
Table S4. Selected bond distances (\AA) and angles (deg) for the calculated (S_0 and T_1 in gas phase and S_0 in CH_2Cl_2) and crystal structures of 2a .	S14
Figure S21. Molecular orbital plots for the optimized structure of A in CH_2Cl_2 solution.	S15
Figure S22. Molecular orbital plots for the optimized structure of 1a in CH_2Cl_2 solution.	S16
Figure S23. Molecular orbital plots for the optimized structure of 1b in CH_2Cl_2 solution.	S17
Figure S24. Molecular orbital plots for the optimized structure of 2a in CH_2Cl_2 solution.	S18
Table S5. The energies of the selected molecular orbitals of A with their compositions in CH_2Cl_2 .	S19
Table S6. The energies of the selected molecular orbitals of 1a with their compositions in CH_2Cl_2 .	S19
Table S7. The energies of the selected molecular orbitals of 1b with their compositions in CH_2Cl_2 .	S20
Table S8. The energies of the selected molecular orbitals of 2a with their compositions in CH_2Cl_2 .	S20
Figure S25. The absorption spectra of A , 1a–b and 2a in CH_2Cl_2 at 298 K (10^{-5} M).	S21
Table S9. The absorption data of A , 1a–b and 2a in CH_2Cl_2 solutions (10^{-5} M).	S21
Table S10. Wavelengths and the nature of transitions for A where $M = \text{Pt}$, $L = \text{dfppy}$, $L' = \text{dmso}$ and $X = \text{Cl}$.	S22
Table S11. Wavelengths and the nature of transitions for 1a where $M = \text{Pt}$, $L = \text{dfppy}$, $L' = \text{PPh}_2\text{py}$ and $X = \text{Cl}$.	S22
Table S12. Wavelengths and the nature of transitions for 1b where $M = \text{Pt}$, $L = \text{dfppy}$, $L' = \text{PPh}_3$ and $X = \text{Cl}$.	S23
Table S13. Wavelengths and the nature of transitions for 2a where $M = \text{Pt}$, $L = \text{ppy}$, $L' = \text{PPh}_2\text{py}$ and $X = \text{Cl}$.	S23
Figure S26. Frontier molecular orbital plots of A , 1a–b and 2a in S_0 and T_1 states and gas phase.	S24
References	S25

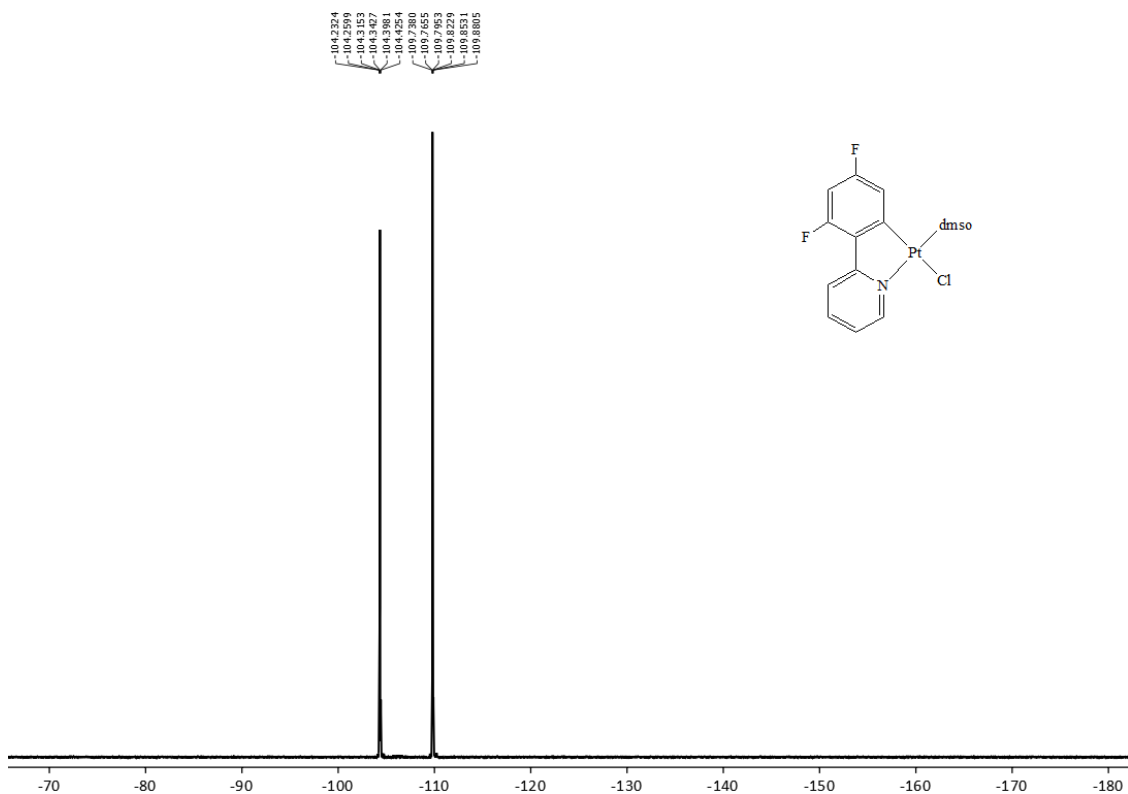
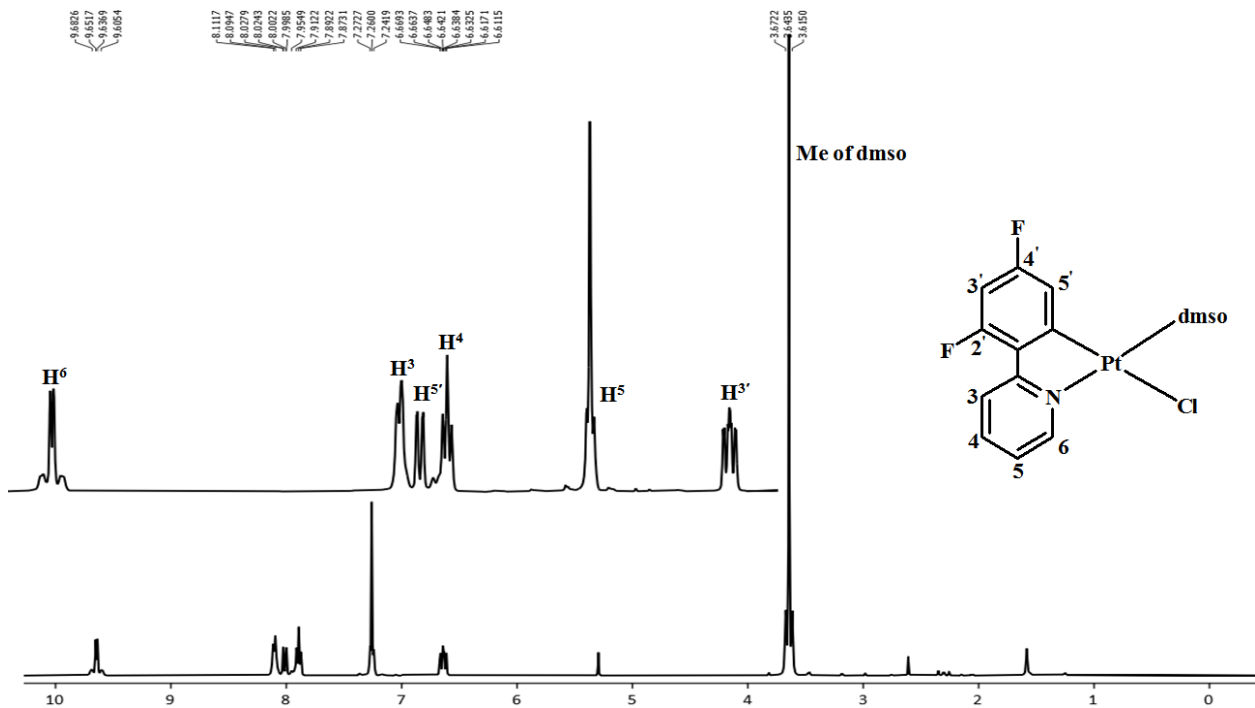


Figure S2. $^{19}\text{F}\{^1\text{H}\}$ NMR spectrum of A in CDCl_3 .

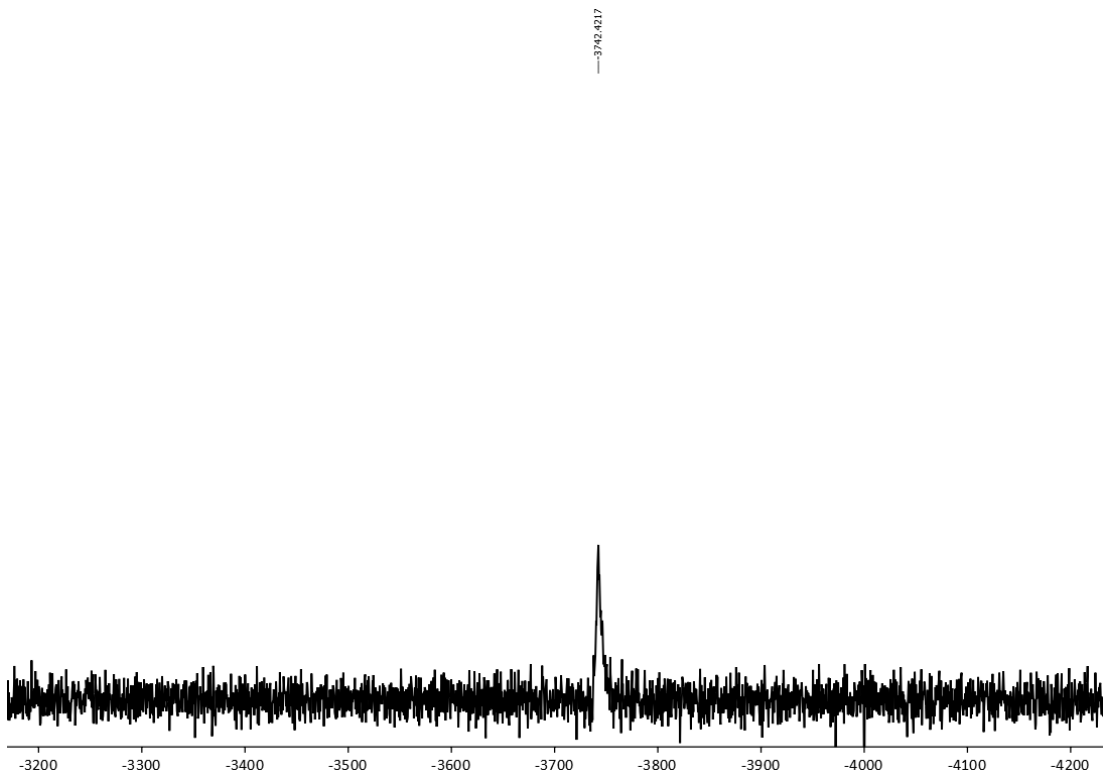


Figure S3. $^{195}\text{Pt}\{\text{H}\}$ NMR spectrum of **A** in CDCl_3 .

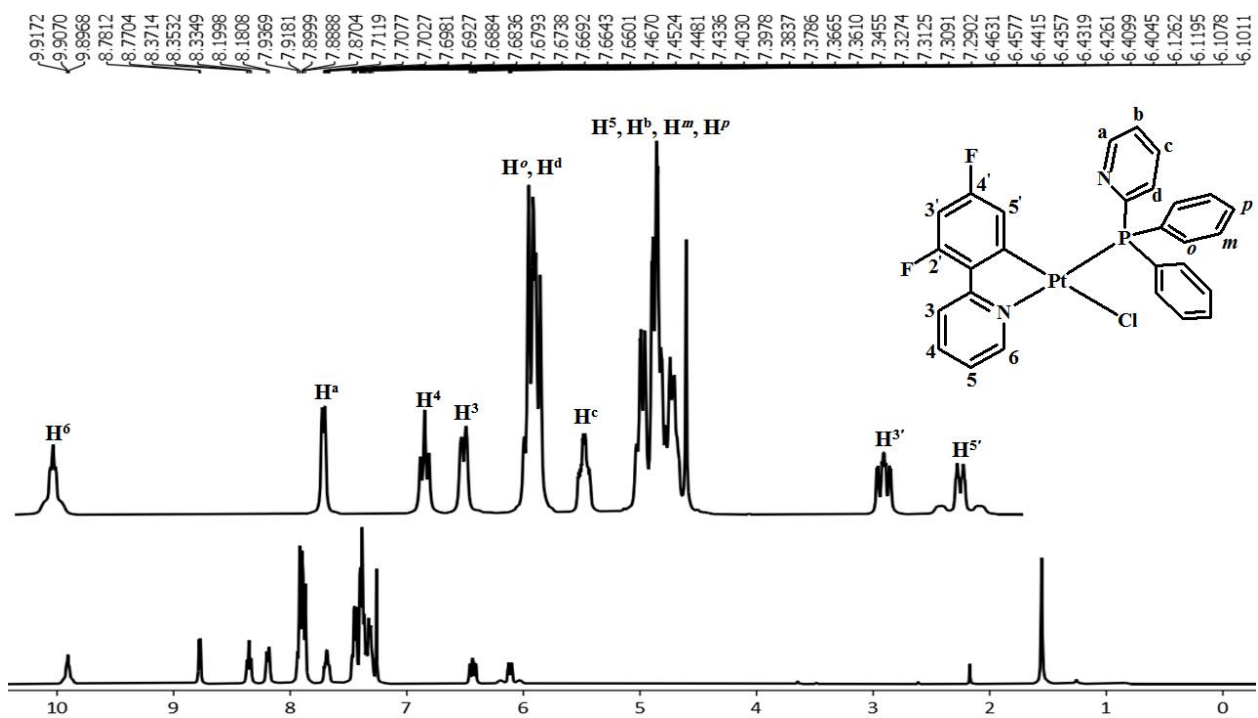


Figure S4. ^1H NMR spectrum of **1a** in CDCl_3 .

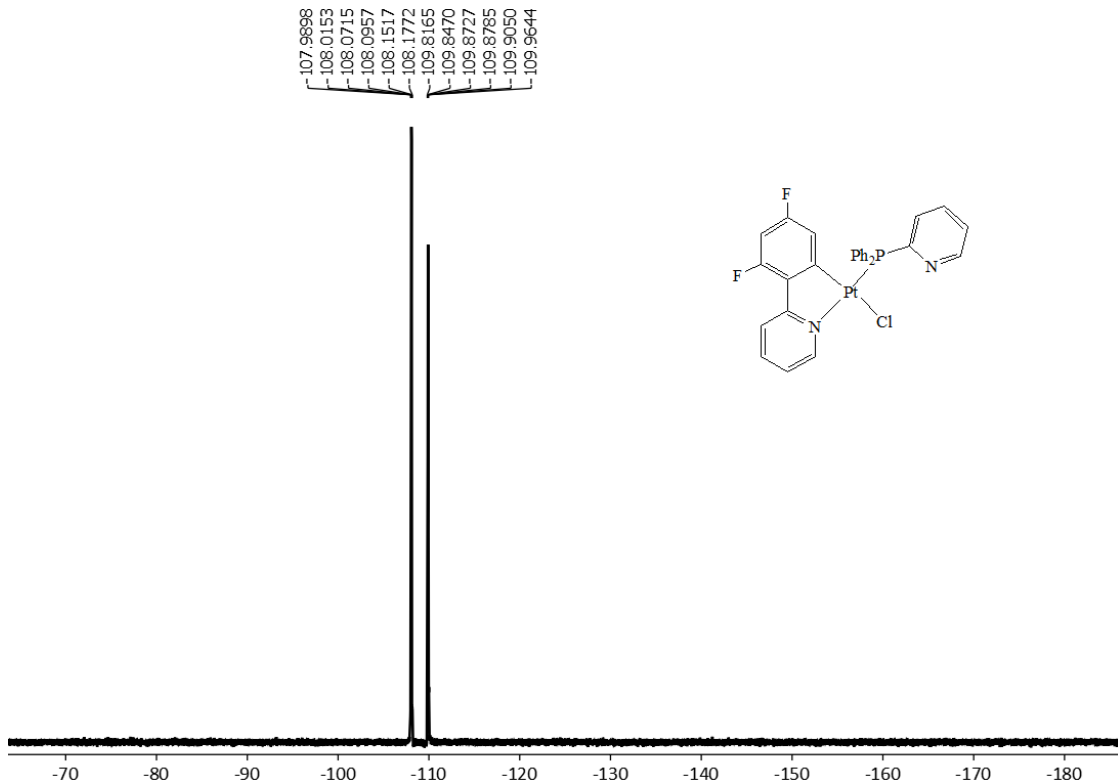


Figure S5. $^{19}\text{F}\{\text{H}\}$ NMR spectrum of **1a** in CDCl_3 .

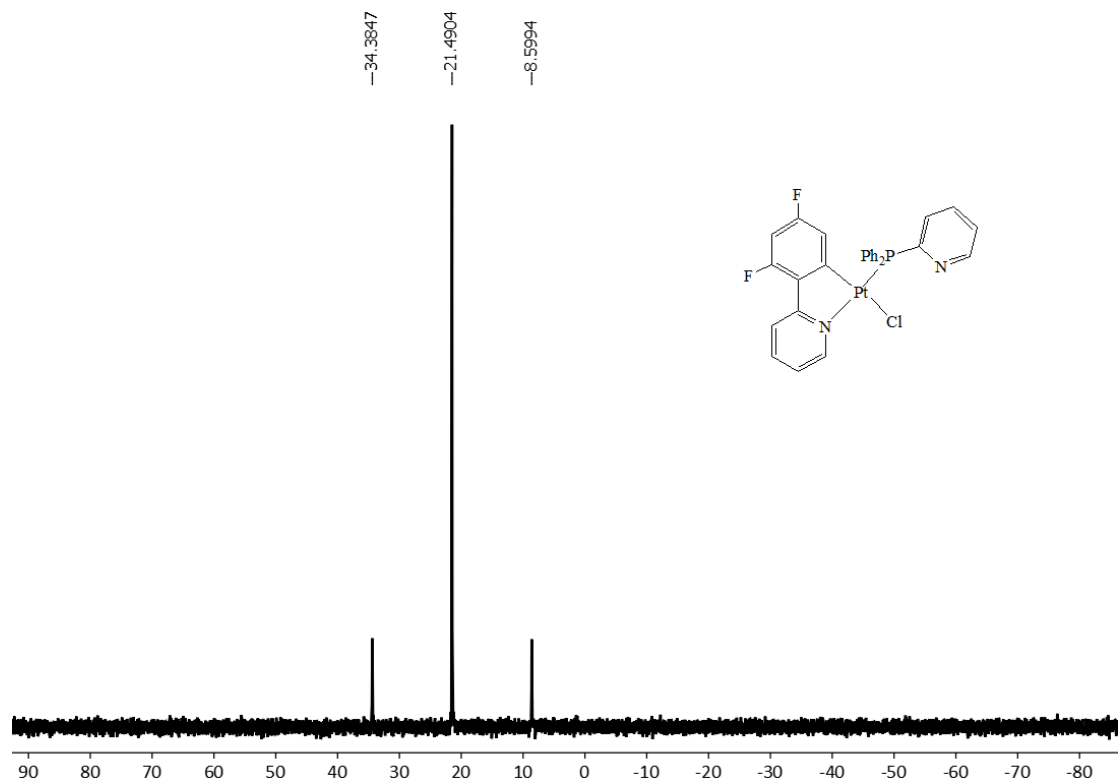


Figure S6. $^{31}\text{P}\{\text{H}\}$ NMR spectrum of **1a** in CDCl_3 .

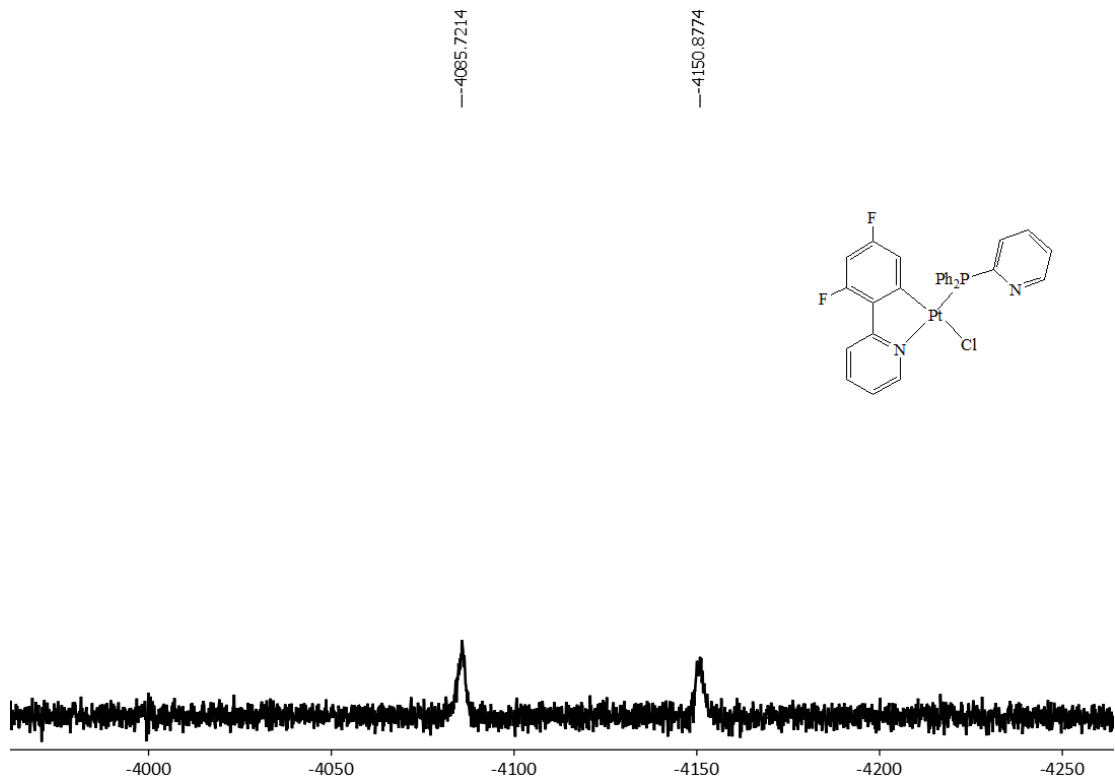


Figure S7. $^{195}\text{Pt}\{\text{H}\}$ NMR spectrum of **1a** in CDCl_3 .

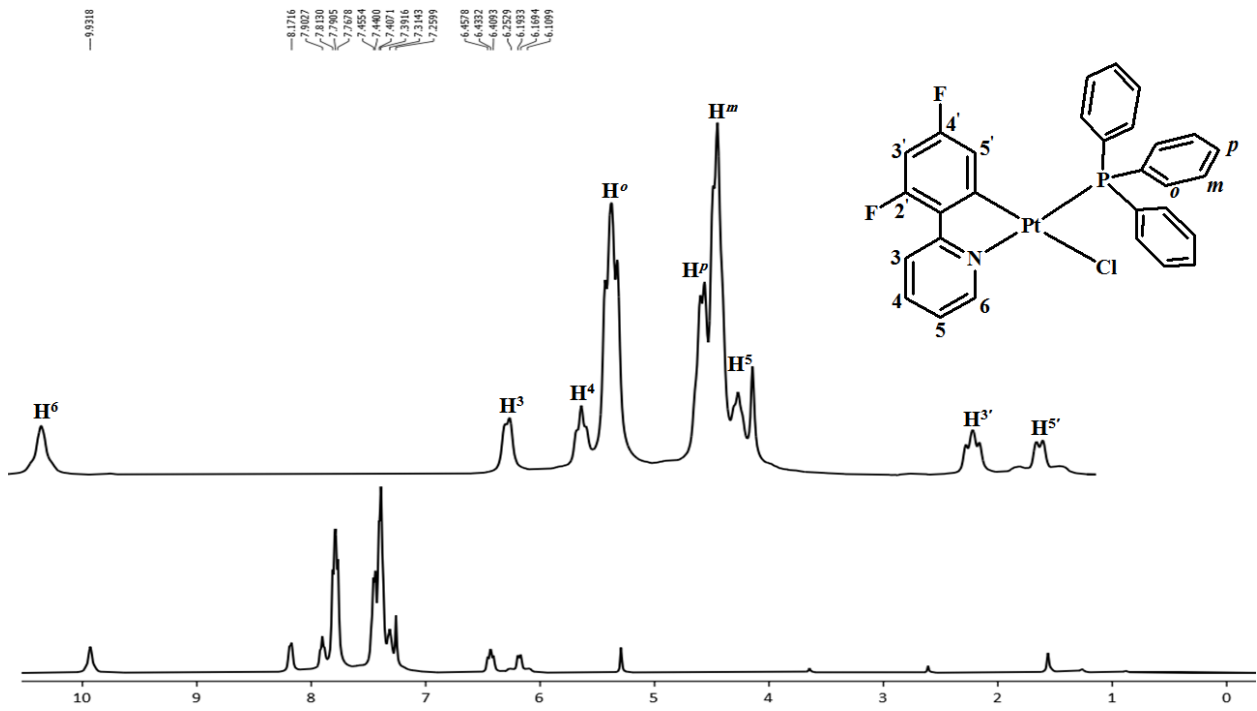


Figure S8. ^1H NMR spectrum of **1b** in CDCl_3 .

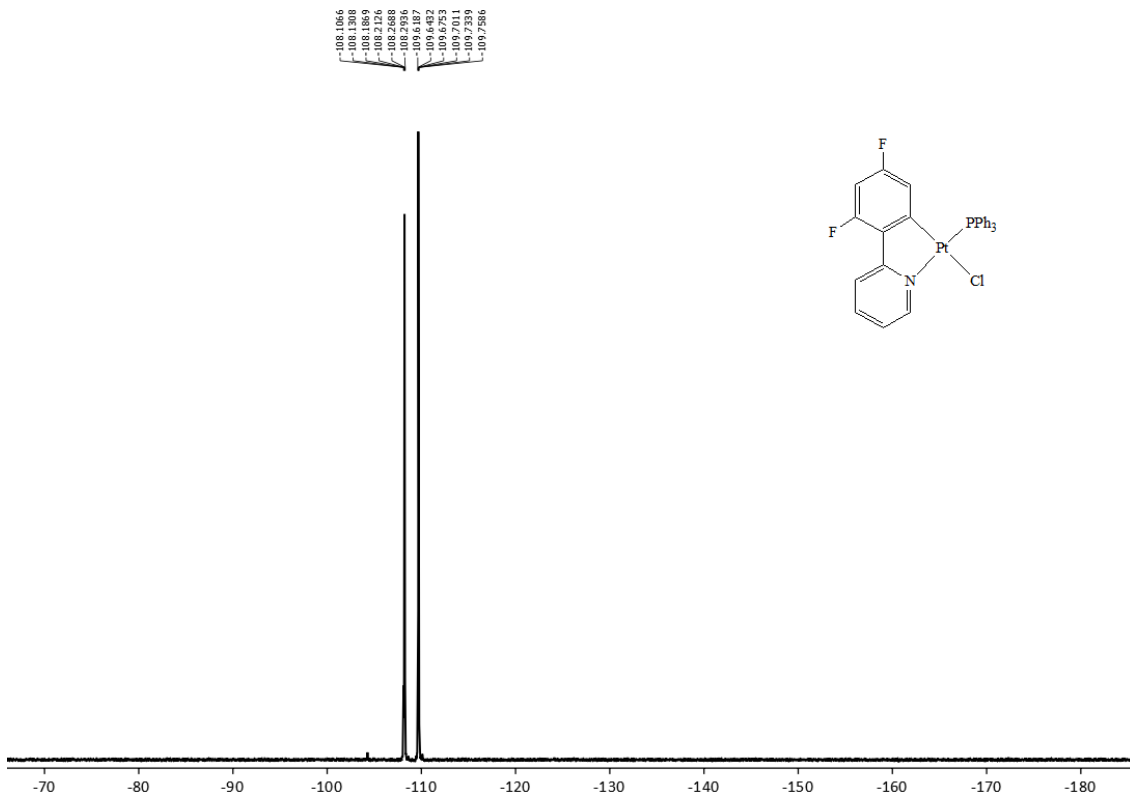


Figure S9. ${}^{19}\text{F}\{{}^1\text{H}\}$ NMR spectrum of **1b** in CDCl_3 .

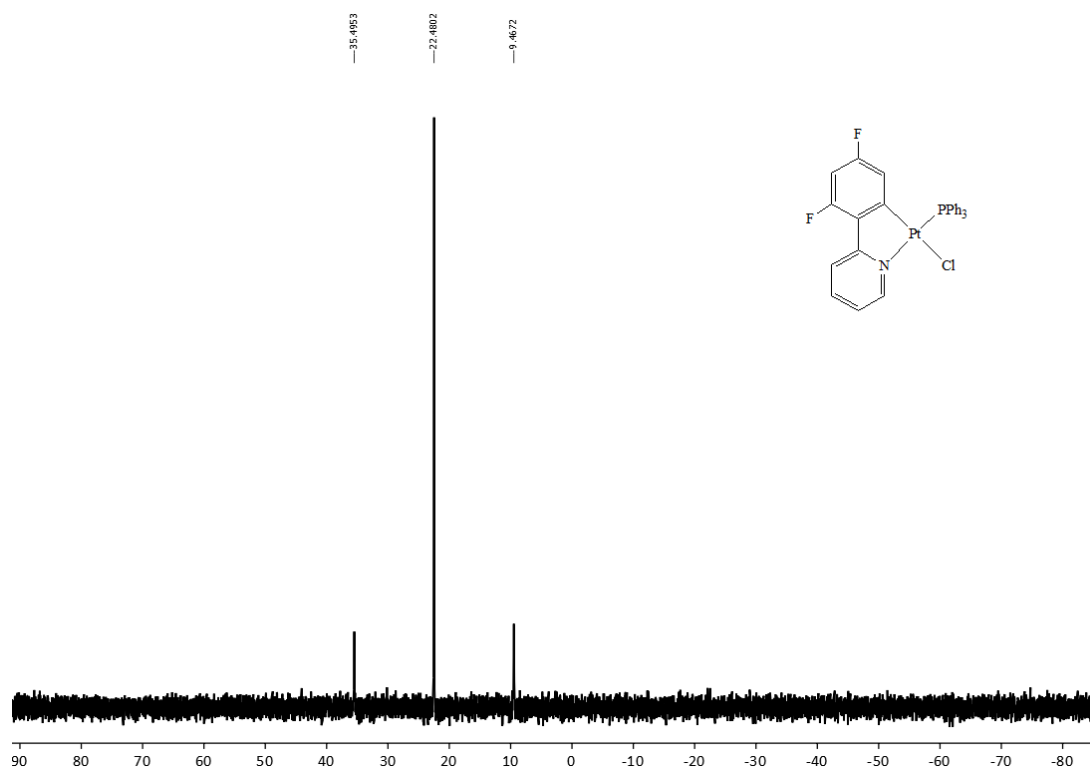


Figure S10. ${}^{31}\text{P}\{{}^1\text{H}\}$ NMR spectrum of **1b** in CDCl_3 .

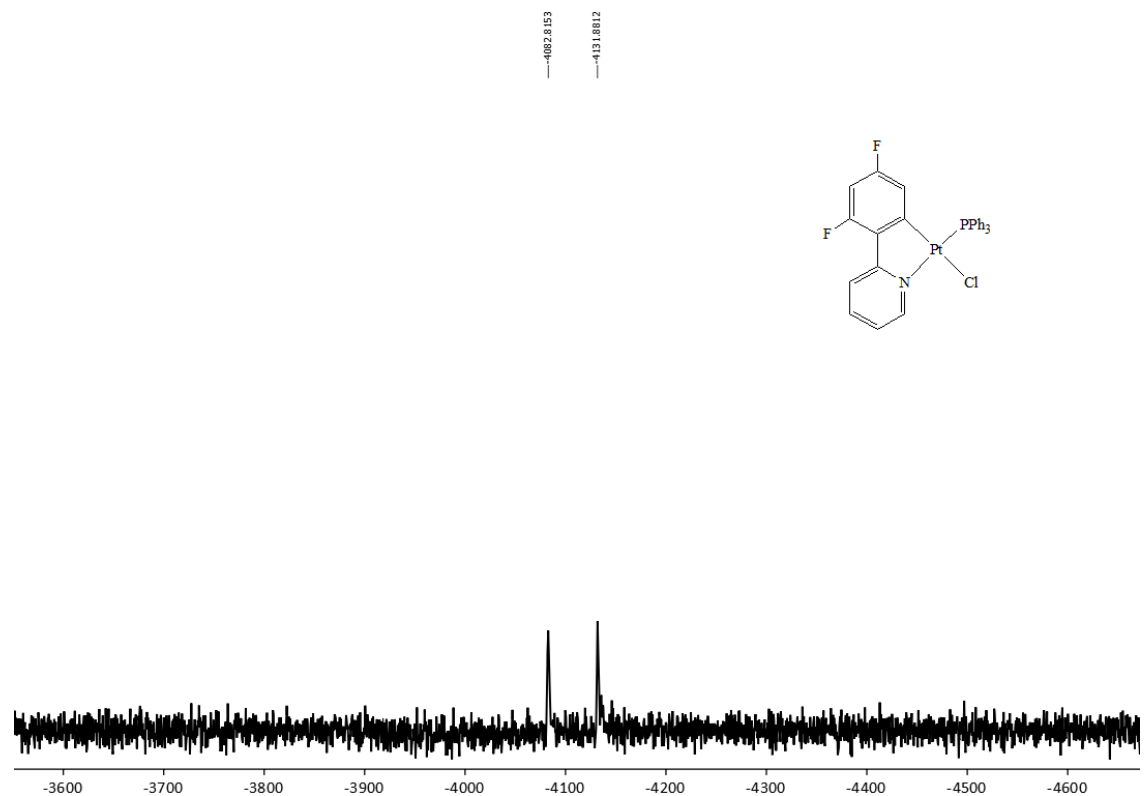


Figure S11. $^{195}\text{Pt}\{\text{H}\}$ NMR spectrum of **1b** in CDCl_3 .

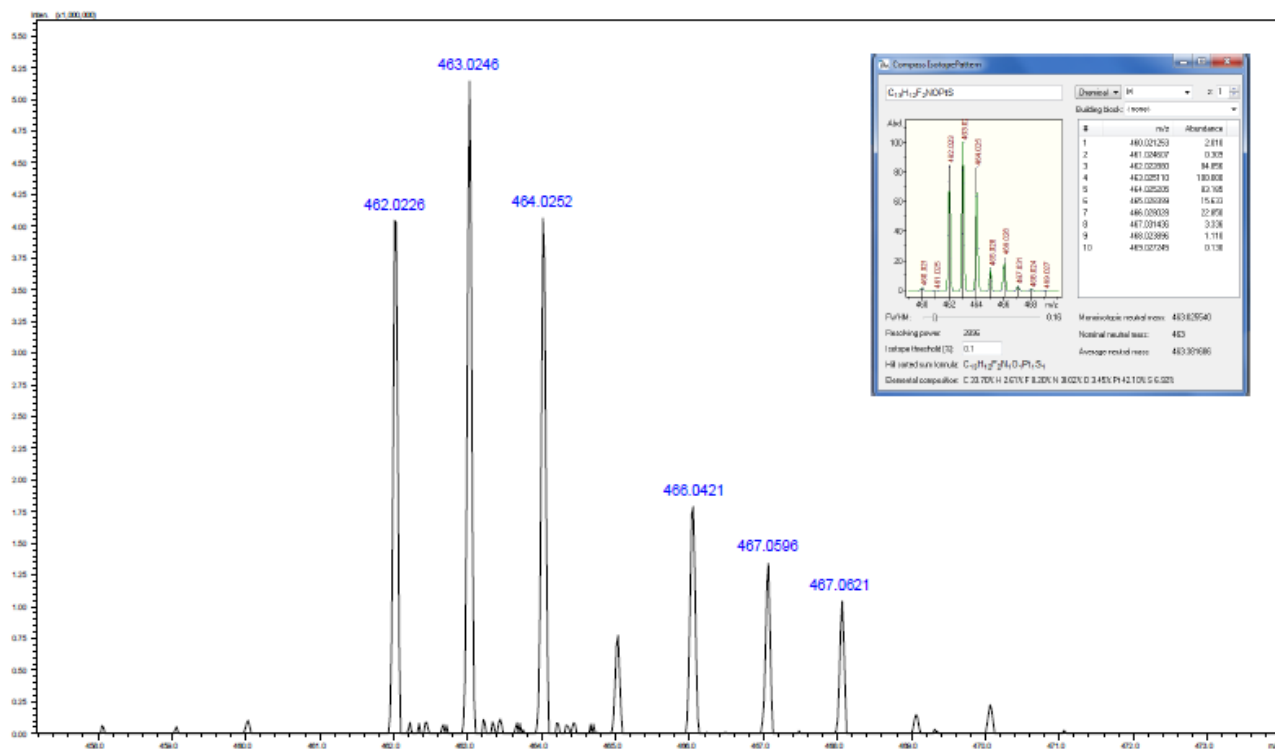


Figure S12. HR ESI-Mass spectrum of **A**. Inset shows the calculated pattern.

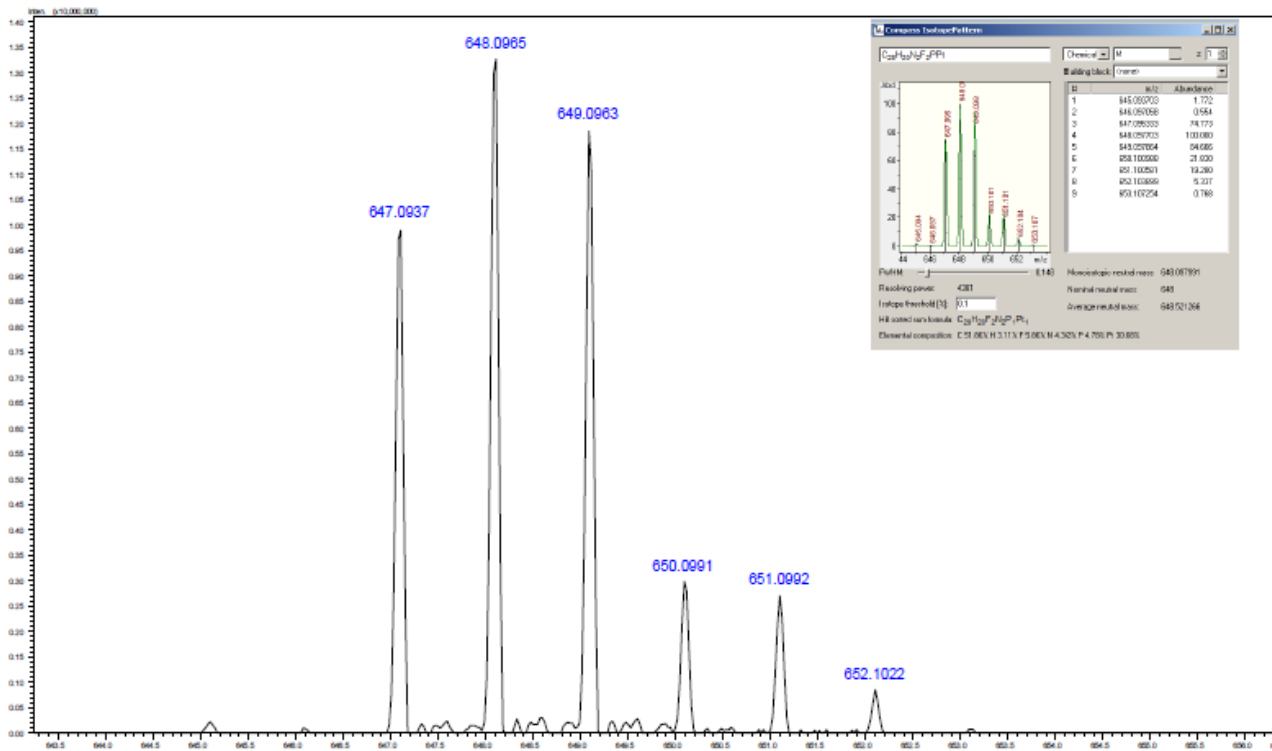


Figure S13. HR ESI-Mass spectrum of **1a**. Inset shows the calculated pattern.

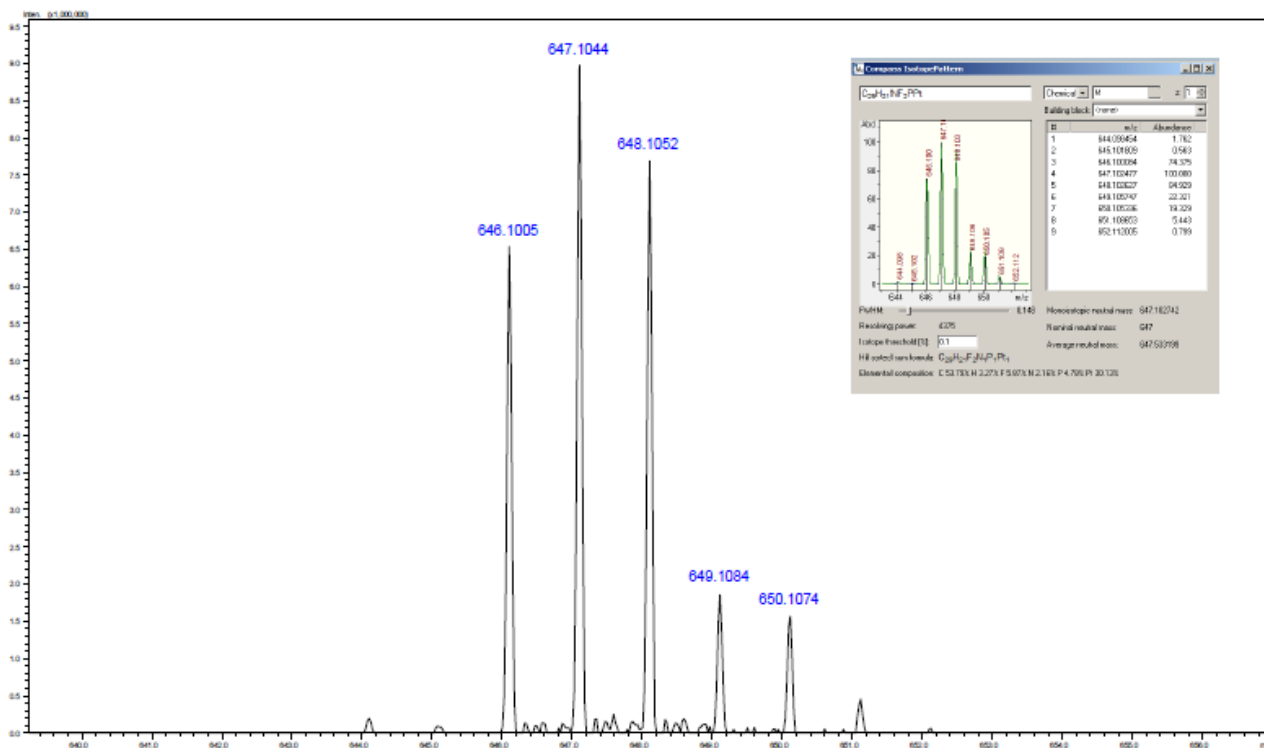


Figure S14. HR ESI-Mass spectrum of **1b**. Inset shows the calculated pattern.

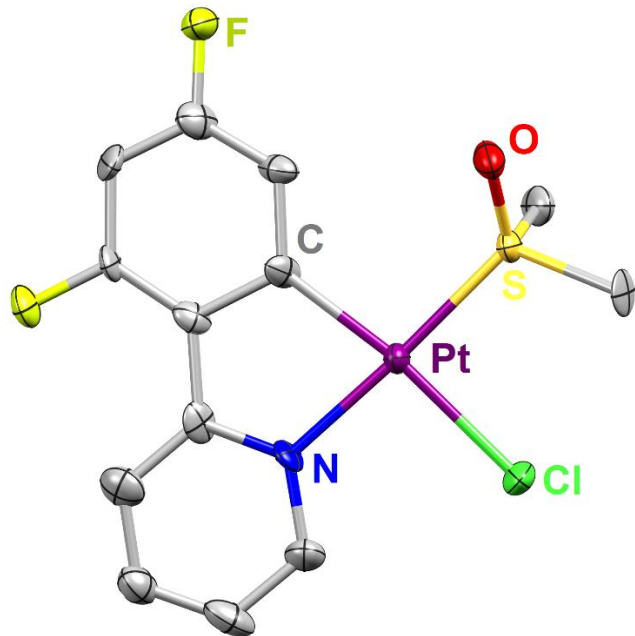


Figure S15. Molecular structure of A.

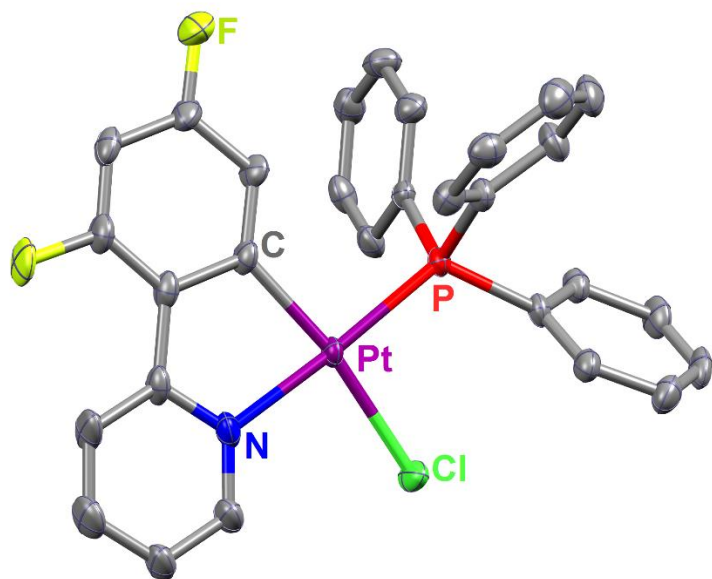


Figure S16. Molecular structure of 1b.

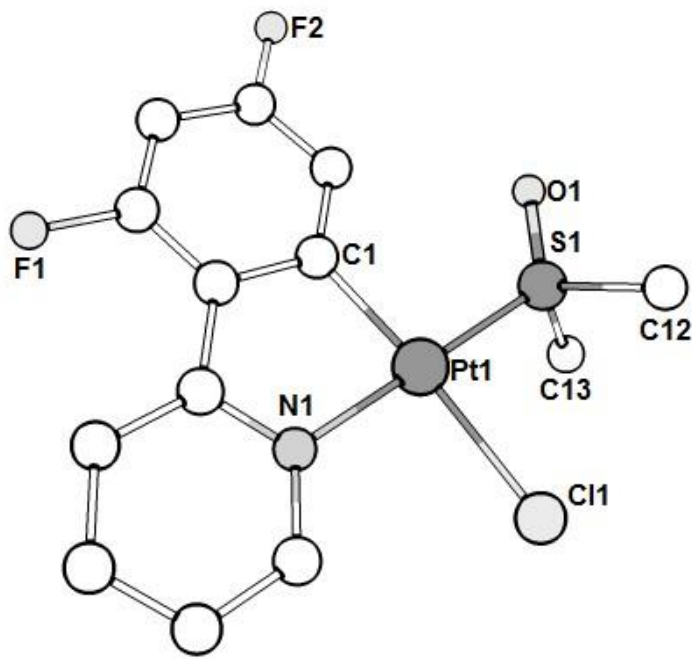


Figure S17. View of the optimized structure of **A** in gas phase (S_0) with atom numbering.

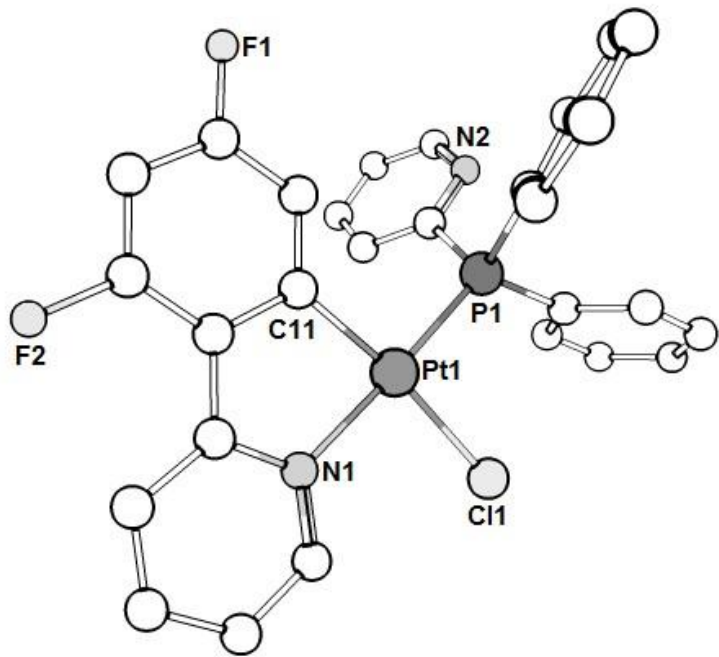


Figure S18. View of the optimized structure of **1a** in gas phase (S_0) with atom numbering.

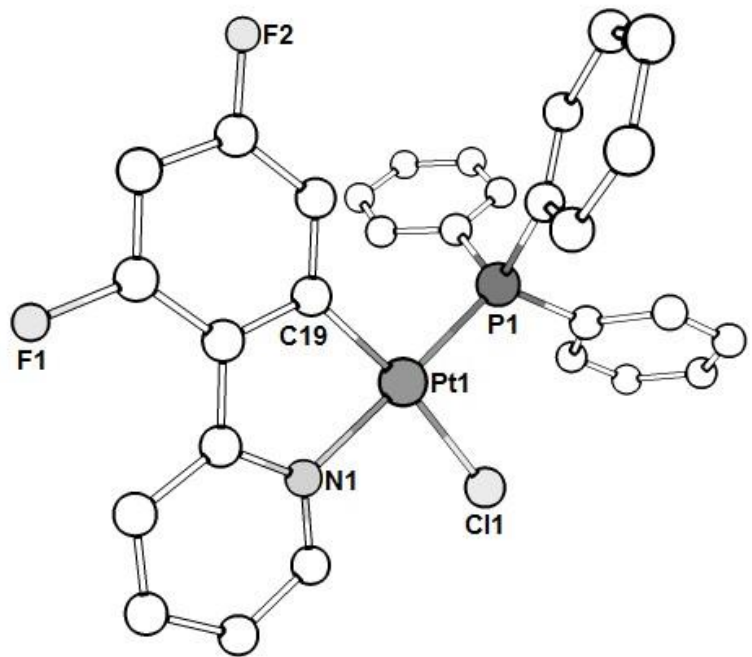


Figure S19. View of the optimized structure of **1b** in gas phase (S_0) with atom numbering.

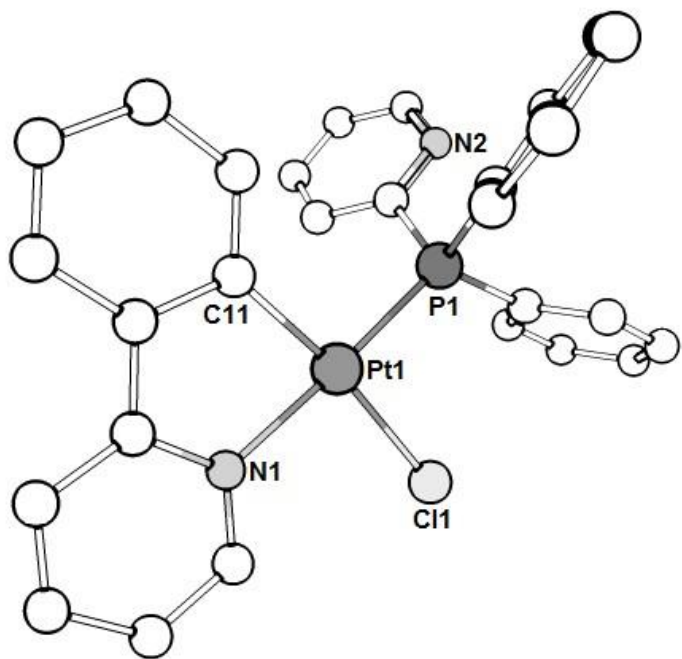


Figure S20. View of the optimized structure of **2a** in gas phase (S_0) with atom numbering.

Table S1. Selected bond distances (\AA) and angles (deg) for the calculated (S_0 and T_1 in gas phase and S_0 in CH_2Cl_2) structures of A.

Bond distance or angle	S_0 (gas phase)	T_1 (gas phase)	S_0 (CH_2Cl_2)
Pt1-C1	2.01693	1.98935	2.01356
Pt1-N1	2.06882	2.03739	2.07494
Pt1-Cl1	2.49854	2.49441	2.52530
Pt1-S1	2.32693	2.34311	2.34527
C1-Pt1-N1	80.53958	81.61921	80.39857
N1-Pt1-Cl1	94.02501	93.66922	94.24241
Cl1-Pt1-S1	86.29798	85.90180	86.31952
S1-Pt1-C1	99.13743	98.80977	99.03949

Table S3. Selected bond distances (\AA) and angles (deg) for the calculated (S_0 and T_1 in gas phase and S_0 in CH_2Cl_2) structures of 1a.

Bond distance or angle	S_0 (gas phase)	T_1 (gas phase)	S_0 (CH_2Cl_2)
Pt1-C11	2.02736	1.99451	2.02736
Pt1-N1	2.11743	2.08554	2.11743
Pt1-Cl1	2.45154	2.44804	2.45154
Pt1-P1	2.30834	2.32712	2.30834
C11-Pt1-N1	80.00244	81.25104	80.00244
N1-Pt1-Cl1	92.29351	91.80313	92.29351
Cl1-Pt1-P1	90.29233	89.75095	90.29233
P1-Pt1-C11	97.41417	97.22065	97.41417

Table S2. Selected bond distances (\AA) and angles (deg) for the calculated (S_0 and T_1 in gas phase and S_0 in CH_2Cl_2) structures of **1b**.

Bond distance or angle	S_0 (gas phase)	T_1 (gas phase)	S_0 (CH_2Cl_2)
Pt1-C19	2.02939	1.99687	2.02463
Pt1-N1	2.11724	2.08444	2.12434
Pt1-Cl1	2.31556	2.45212	2.49718
Pt1-P1	2.31556	2.33505	2.32777
C19-Pt1-N1	79.93027	81.19505	79.95225
N1-Pt1-Cl1	91.74376	91.26690	91.85467
Cl1-Pt1-P1	90.39175	89.85544	91.03254
P1-Pt1-C19	97.93343	97.68197	97.17647

Table S4. Selected bond distances (\AA) and angles (deg) for the calculated (S_0 and T_1 in gas phase and S_0 in CH_2Cl_2) and crystal structures of **2a**.

Bond distance or angle	S_0 (gas phase)	Crystal Structure	T_1 (gas phase)	S_0 (CH_2Cl_2)
Pt1-C11	2.03101	1.989	1.98836	2.03101
Pt1-N1	2.12203	2.112	2.09017	2.12203
Pt1-Cl1	2.45992	2.383	2.45101	2.45992
Pt1-P1	2.30086	2.222	2.32736	2.30086
C11-Pt1-N1	80.01041	80.98	81.48354	80.01041
N1-Pt1-Cl1	91.82854	92.50	91.52863	91.82854
Cl1-Pt1-P1	90.85784	92.13	89.95885	90.85784
P1-Pt1-C11	97.30739	94.62	97.07743	97.30739

The crystal structure of **2a** has been previously reported and brought here for comparison.¹

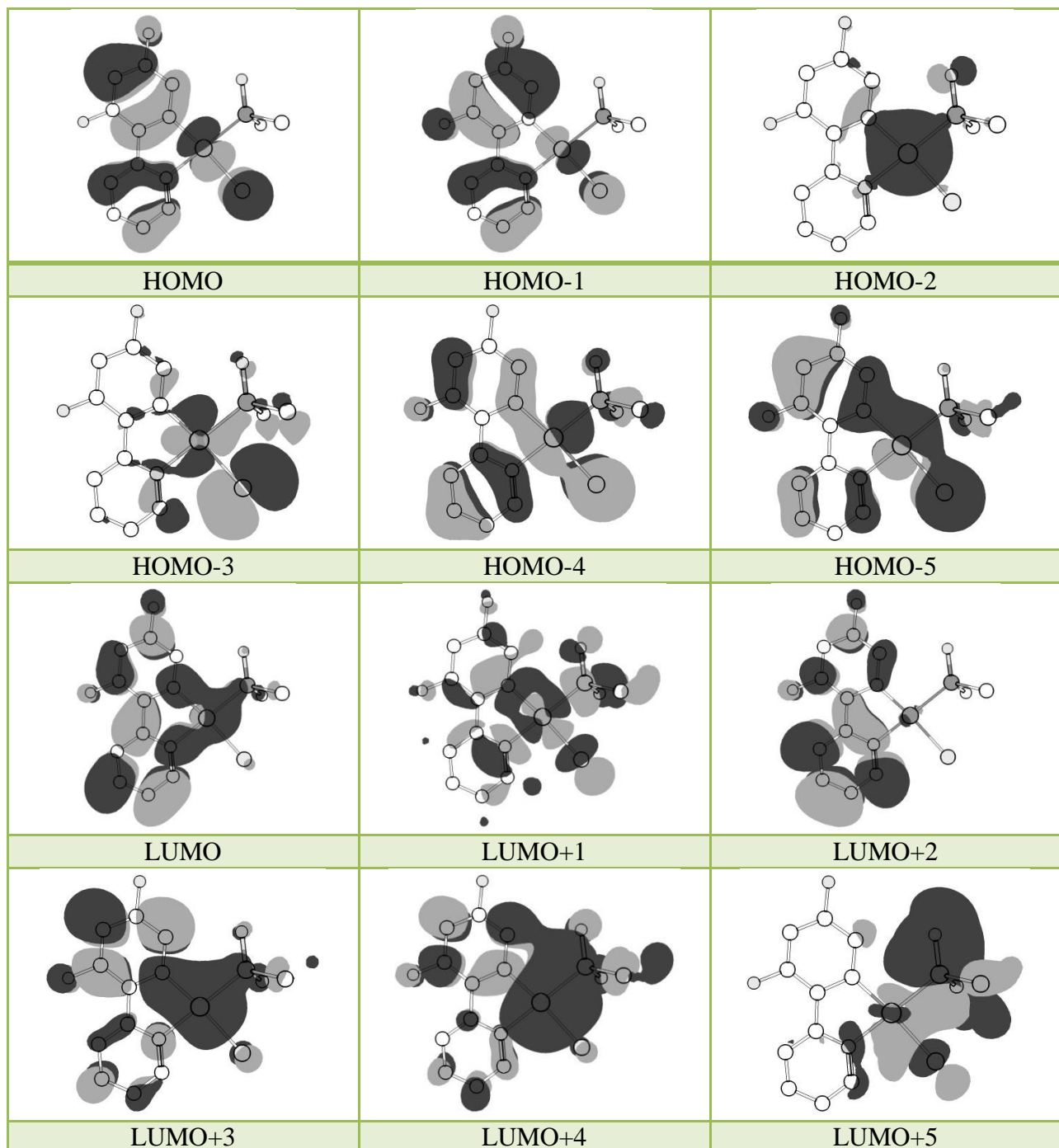


Figure S21. Molecular orbital plots for the optimized structure of **A** in CH₂Cl₂ solution.

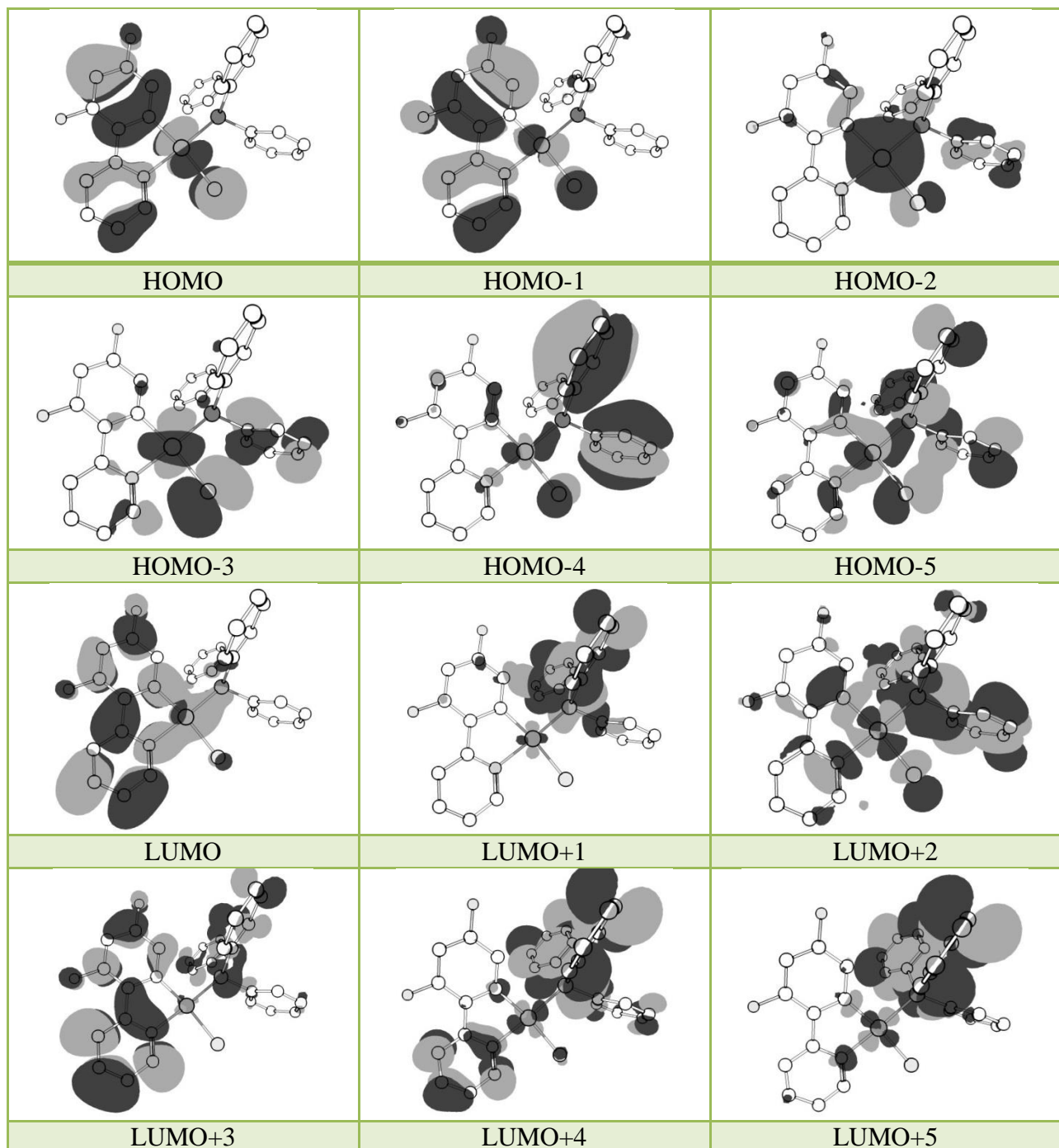


Figure S22. Molecular orbital plots for the optimized structure of **1a** in CH₂Cl₂ solution.

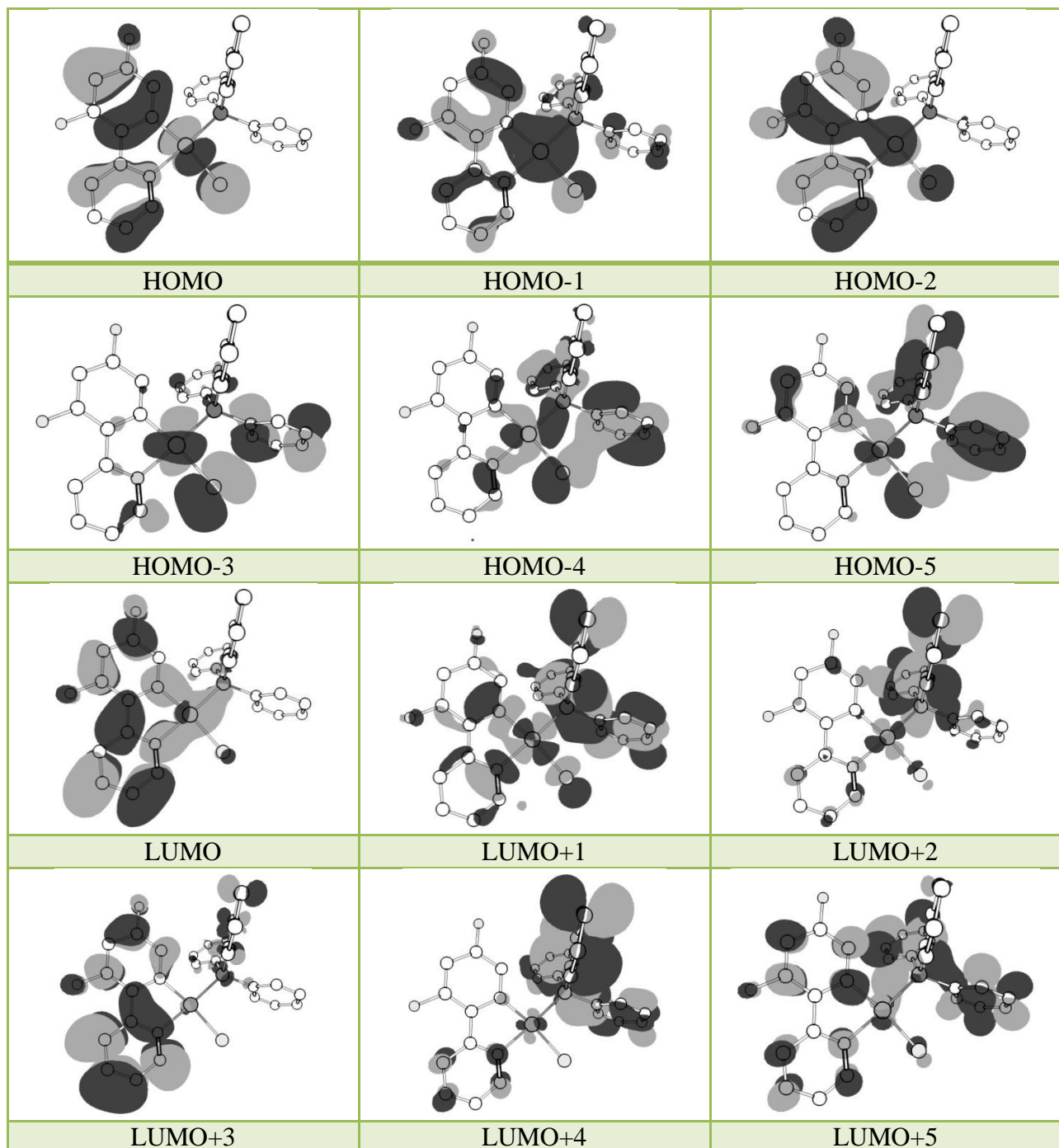


Figure S23. Molecular orbital plots for the optimized structure of **1b** in CH₂Cl₂ solution.

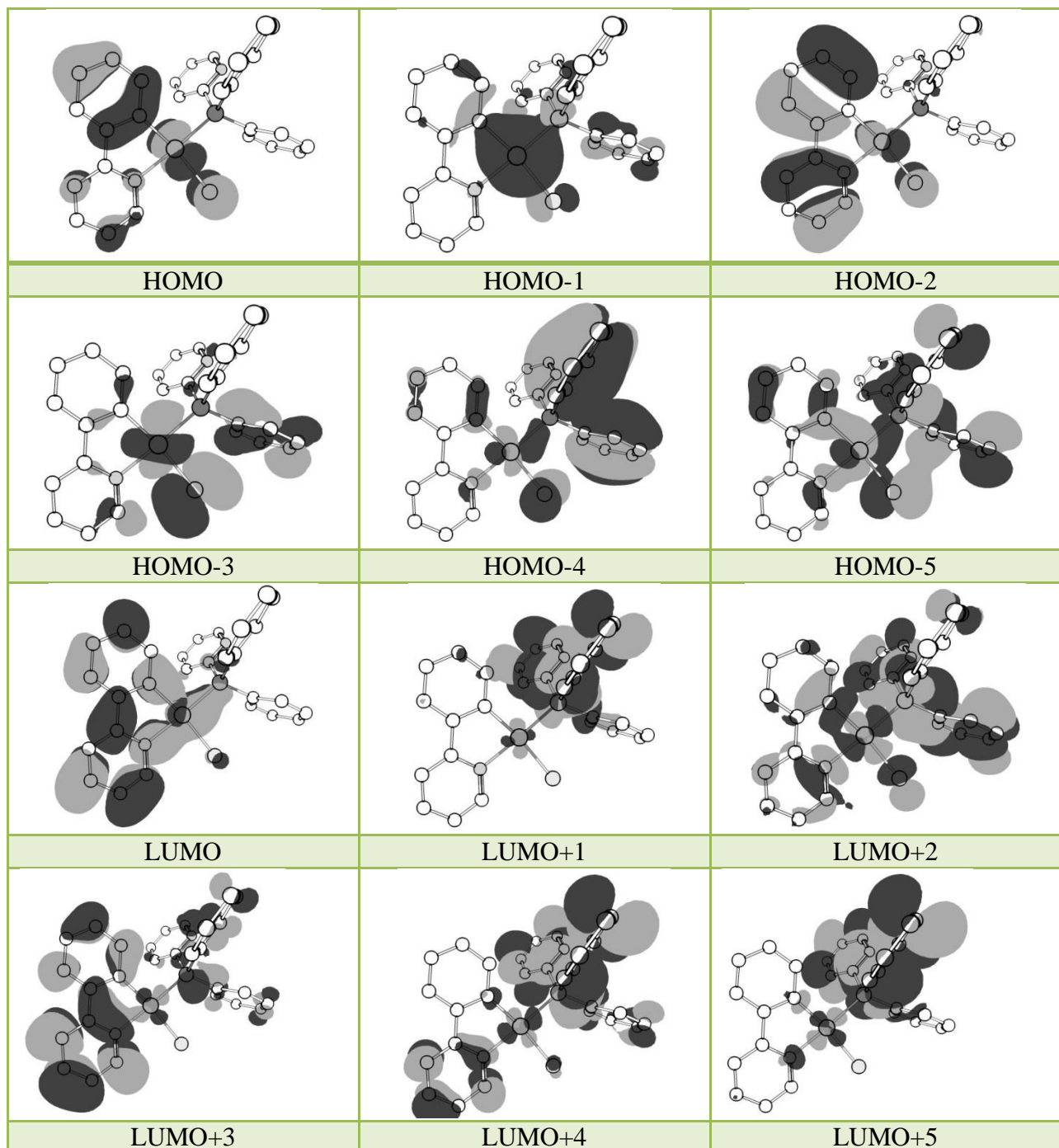


Figure S24. Molecular orbital plots for the optimized structure of **2a** in CH₂Cl₂ solution.

Table S5. The energies of the selected molecular orbitals of **A** with their compositions in CH₂Cl₂.

MO	Energy (eV)	A			
		Pt	dfppy	Cl	dmso
LUMO+5	0.357	22	11	5	62
LUMO+4	0.357	23	28	1	48
LUMO+3	-0.381	15	71	1	13
LUMO+2	-1.108	1	98	0	1
LUMO+1	-1.243	37	27	6	30
LUMO	-1.964	6	88	1	5
HOMO	-6.171	39	48	12	0
HOMO-1	-6.536	12	82	6	0
HOMO-2	-6.701	91	6	0	3
HOMO-3	-7.145	22	6	69	3
HOMO-4	-7.307	49	23	23	5
HOMO-5	-7.443	38	26	32	4

Table S6. The energies of the selected molecular orbitals of **1a** with their compositions in CH₂Cl₂.

MO	Energy (eV)	1a			
		Pt	dfppy	Cl	PPh ₂ py
LUMO+5	-0.666	3	5	1	91
LUMO+4	-0.851	4	16	1	79
LUMO+3	-1.012	1	80	0	19
LUMO+2	-1.143	29	16	5	49
LUMO+1	-1.404	2	3	0	95
LUMO	-1.813	6	87	1	6
HOMO	-6.000	43	39	17	1
HOMO-1	-6.455	10	81	6	3
HOMO-2	-6.495	81	5	3	11
HOMO-3	-6.651	23	5	52	20
HOMO-4	-6.920	3	4	5	88
HOMO-5	-6.991	21	8	15	56

Table S7. The energies of the selected molecular orbitals of **1b** together with their compositions in CH₂Cl₂.

MO	Energy (eV)	1b			
		Pt	dfppy	Cl	PPh ₃
LUMO+5	-0.576	6	16	1	77
LUMO+4	-0.733	2	6	0	92
LUMO+3	-0.992	1	90	0	9
LUMO+2	-1.084	3	4	1	92
LUMO+1	-1.232	31	18	4	46
LUMO	-1.814	6	88	1	6
HOMO	-5.998	44	38	17	1
HOMO-1	-6.419	69	17	3	11
HOMO-2	-6.461	28	64	5	3
HOMO-3	-6.608	20	5	52	23
HOMO-4	-6.944	20	8	15	57
HOMO-5	-6.969	7	6	16	72

Table S8. The energies of the selected molecular orbitals of **2a** with their compositions in CH₂Cl₂.

MO	Energy (eV)	2a			
		Pt	ppy	Cl	PPh ₂ py
LUMO+5	-0.615	3	4	0	93
LUMO+4	-0.825	4	12	1	83
LUMO+3	-1.031	4	77	1	18
LUMO+2	-1.051	27	16	4	53
LUMO+1	-1.371	1	3	1	95
LUMO	-1.746	5	88	1	6
HOMO	-5.811	45	39	15	1
HOMO-1	-6.397	83	5	2	10
HOMO-2	-6.464	8	83	6	3
HOMO-3	-6.589	22	5	56	16
HOMO-4	-6.879	6	5	8	81
HOMO-5	-6.924	18	10	15	57

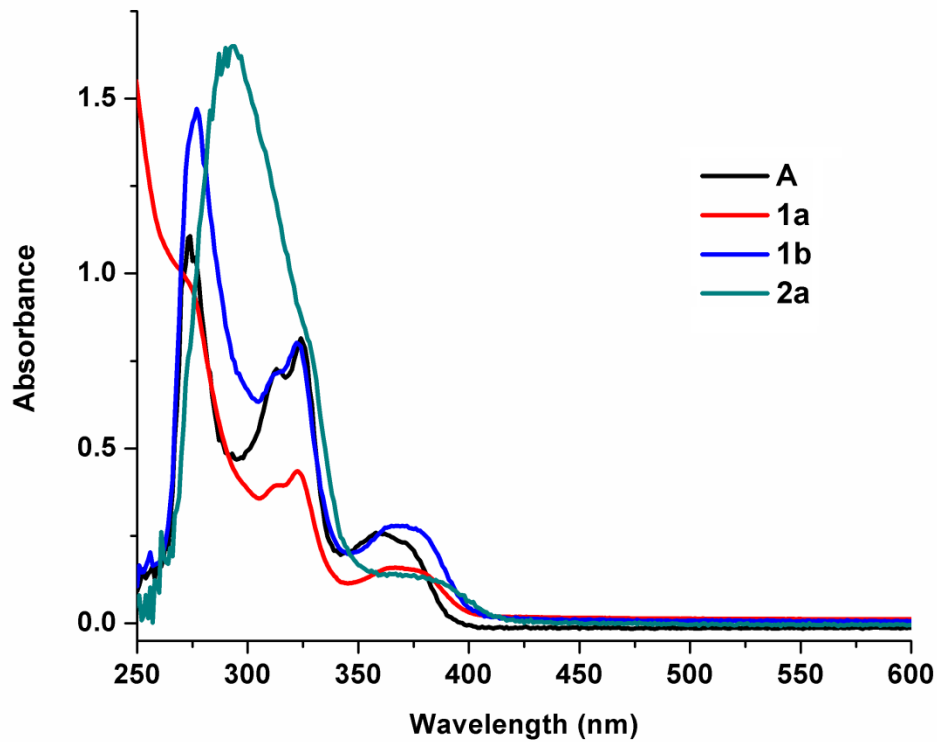


Figure S25. The absorption spectra of **A**, **1a–b** and **2a** in CH_2Cl_2 at 298 K (10^{-5} M).

Table S9. The absorption data of **A**, **1a–b** and **2a** in CH_2Cl_2 solutions (10^{-5} M).

Complex	Absorption / nm ($10^5 \epsilon/\text{M}^{-1} \text{cm}^{-1}$)
A	360 (0.279), 323 (0.823), 312 (0.741), 273 (1.128)
1a	370 (0.172), 323 (0.449), 312 (0.417), 272 (0.991)
1b	371 (0.291), 323 (0.828), 312 (0.735), 276 (1.480)
2a	377 (0.138), 327 (0.849), 293 (1.660)

Table S10. Wavelengths and the nature of transitions for **A** where M = Pt, L = dfppy, L' = dmso and X = Cl.

Excited state	Oscillator strength	Calculated λ (nm)	Transitions (Major Contribution)	Assignment
S ₀ →S ₁	0.0486	359.75	HOMO→LUMO (95%)	ILCT/MLCT/XLCT
S ₀ →S ₅	0.1830	309.91	H-1→LUMO (82%)	ILCT/MLCT
S ₀ →S ₆	0.1139	283.70	HOMO→L+2 (79%)	ILCT/MLCT/XLCT
			H-4→LUMO (14%)	MLCT/ILCT/XLCT
S ₀ →S ₁₀	0.1407	269.46	H-4→LUMO (56%)	MLCT/ILCT/XLCT
			H-1→L+2 (16%)	ILCT/MLCT
			H-5→LUMO (11%)	MLCT/ILCT/XLCT
			HOMO→L+2 (10%)	ILCT/MLCT/XLCT

Table S11. Wavelengths and the nature of transitions for **1a** where M = Pt, L = dfppy, L' = PPh₂py and X = Cl.

Excited state	Oscillator strength	Calculated λ (nm)	Transitions (Major Contribution)	Assignment
S ₀ →S ₁	0.0571	360.97	HOMO→LUMO (97%)	ILCT/MLCT/XLCT
S ₀ →S ₅	0.0617	308.30	H-1→LUMO (49%)	ILCT
			H-2→L+2 (29%)	ML'CT/MLCT
S ₀ →S ₆	0.0924	303.40	H-2→L+2 (46%)	ML'CT/MLCT
			H-1→LUMO (29%)	ILCT
S ₀ →S ₈	0.0502	287.49	HOMO→L+3 (76%)	ILCT/MLCT/XLCT/ML'CT
S ₀ →S ₁₁	0.0176	275.08	H-1→L+1 (89%)	LL'CT

Table S12. Wavelengths and the nature of transitions for **1b** where M = Pt, L = dfppy, L' = PPh₃ and X = Cl.

Excited state	Oscillator strength	Calculated λ (nm)	Transitions (Major Contribution)	Assignment
S ₀ →S ₁	0.0565	361.79	HOMO→LUMO (96%)	ILCT/MLCT/XLCT
S ₀ →S ₅	0.1460	306.45	H-2→LUMO (68%)	ILCT/MLCT
			H-1→LUMO (15%)	MLCT/ILCT
S ₀ →S ₁₁	0.2361	275.96	H-6→LUMO (56%)	MLCT/L'LCT/ILCT
			HOMO→L+3 (11%)	ILCT/MLCT/XLCT

Table S13. Wavelengths and the nature of transitions for **2a** where M = Pt, L = ppy, L' = PPh₂py and X = Cl.

Excited state	Oscillator strength	Calculated λ (nm)	Transitions (Major Contribution)	Assignment
S ₀ →S ₁	0.0595	373.47	HOMO→LUMO (98%)	ILCT/MLCT/XLCT
S ₀ →S ₅	0.0267	306.60	HOMO→L+3 (45%)	ILCT/MLCT/ML'CT
			H-2→LUMO (39%)	ILCT
S ₀ →S ₈	0.1758	295.09	H-2→LUMO (52%)	ILCT
			HOMO→L+3 (25%)	ILCT/MLCT/ML'CT
S ₀ →S ₁₂	0.1820	274.60	H-6→LUMO (37%)	L'LCT/MLCT
			H-7→LUMO (28%)	MLCT/L'LCT/ILCT/XLCT

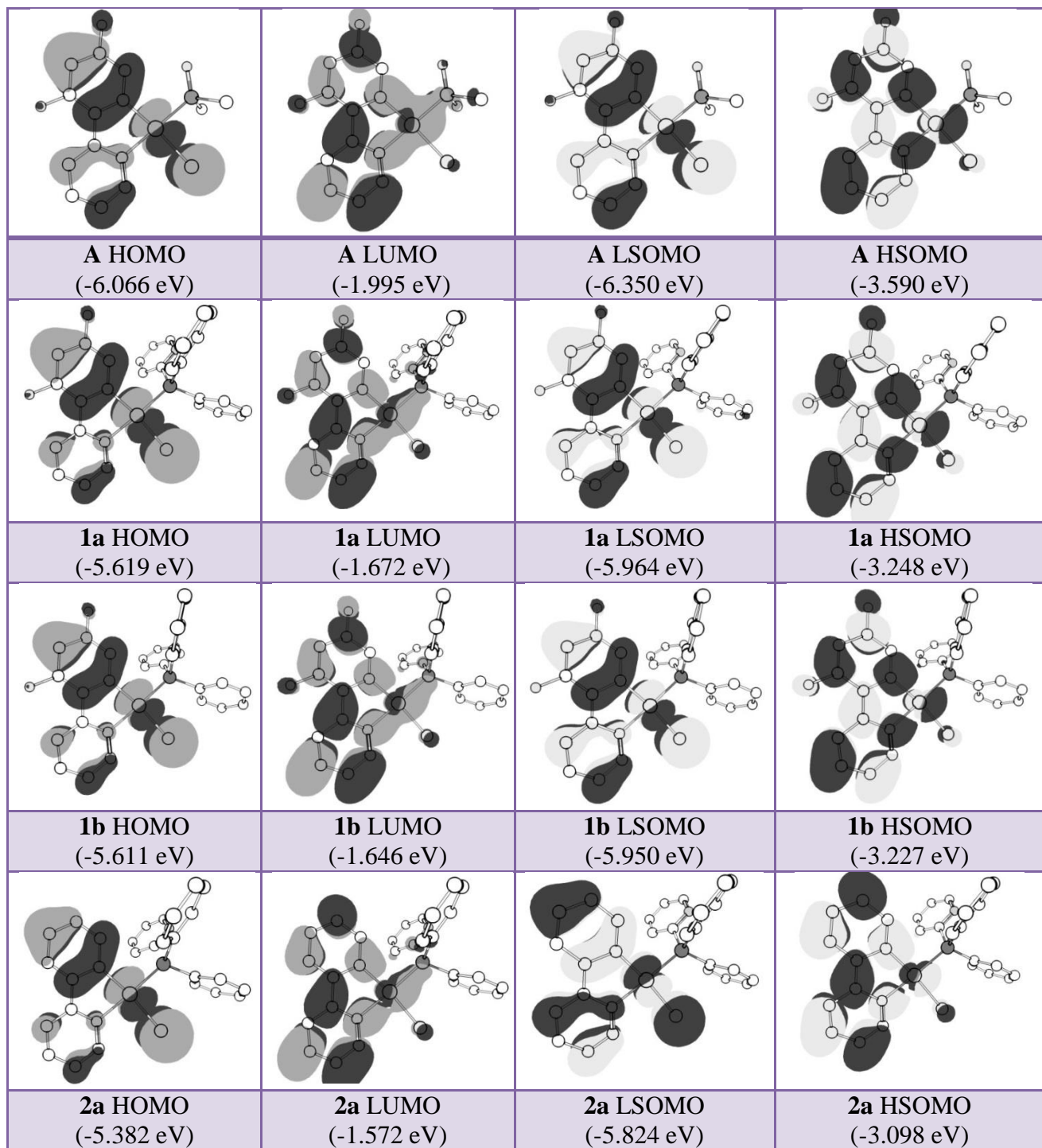


Figure S26. Frontier molecular orbital plots of **A**, **1a–b** and **2a** in S_0 and T_1 states and gas phase.

References

1. M. Fereidoonnezhad, M. Niazi, Z. Ahmadipour, T. Mirzaee, Z. Faghah, Z. Faghah and H. R. Shahsavari, *Eur. J. Inorg. Chem.*, 2017, 2247-2254.